Electronic Supplementary Information

Experimental Section

Materials: $CoCl_2·6H_2O$, $NiCl_2·6H_2O$, hexadecyl trimethyl ammonium bromide were purchased from Aladdin Ltd (China). Urea was purchased from Beijing Chemical Corp. $K_2B_4O_7·4H_2O$ and KOH were provided by Chengdu Kelong Chemical Reagent Factory. $RuCl_3·3H_2O$ was purchased from Sigma-Aldrich Chemical Reagent Co., Ltd. Carbon cloth (CC) was bought from Hongshan District, Wuhan Instrument Surgical Instruments business, and treated in nitric acid (HNO_3) to serve as substrate for active materials. All chemical regents were used as received without further purification. Deionized water was made by the Millipore system and used in all experimental process.

Synthesis of $NiCo_2O_4$/CC and $NiCo_2O_4$@Ni-Co-B/CC: $NiCo_2O_4$/CC was prepared as follows. 1.289 g $CoCl_2·6H_2O$, 0.643 g $NiCl_2·6H_2O$, 0.729 g hexadecyl trimethyl ammonium bromide, 0.54 g urea are dissolved into 50 ml deionized water to form a transparent pink solution. After putting a piece of cleaned CC, the solution was then transferred to a Teflon-lined stainless steel autoclave and kept at 100 °C for 6 h. The CC covered with NiCo-precursor was carefully cleaned for several times with deionized water and ethanol. And it was finally dried in air. Then, the sample was calcined at 300 °C under Ar atomosphere for 3 h to get well defined crystallized $NiCo_2O_4$. To prepare $NiCo_2O_4$@Ni-Co-B/CC, the resulting $NiCo_2O_4$/CC was submitted to oxidative polarization at overpotential of 370 mV vs. RHE in 0.1 M K-Bi for 50 min in a standard three-electrode system (Ag/AgCl as the reference electrode , platinum wire as the counter electrode and $NiCo_2O_4$/CC as the working electrode).

Synthesis of RuO_2/CC: RuO_2 was prepared in accordance with previous report.[1] Briefly, 2.61 g of $RuCl_3·3H_2O$ and 1.0 mL NaOH (1.0 M) were mixed with 100 ml deionized water. Then the solution was stirred for 45 min at 100 °C. After centrifugation, the resulting RuO_2 was collected and washed with water for several times. Finally, the resulting sample was dried at 80 °C for 24 h and annealed at 300 °C in air for 3 h. 20 mg RuO_2 and 10 μL 5 wt% Nafion solution were dispersed in 990 μL water/ethanol (V:V = 1:1) by 30 min sonication to form a catalyst ink. Then 115 μL catalyst ink was loaded on CC with a loading mass of ~2.3 mg cm^{-2}.

Characterizations: XRD data were collected on a Rigaku X-ray diffractometer equipped with a Cu Kα radiation source. SEM measurements were performed on a Hitachi S-4800 field emission scanning electron microscope at an accelerating voltage of 20 kV. TEM measurements were carried out on a Zeiss Libra 200FE transmission electron microscope operated at 200 kV. XPS data were collected on an ESCALABMK II X-ray photoelectron spectrometer using Mg as the exciting source.

Electrochemical measurements: Electrochemical measurements were performed with a CHI 660E electrochemical analyzer (CH Instruments, Inc., Shanghai) in a standard three-electrode system using a $NiCo_2O_4$@Ni-Co-B/CC as the working electrode, a platinum wire as the counter electrode and Hg/HgO as the reference electrode. The potentials reported in this work were calibrated to reversible hydrogen electrode (RHE), using the following equation: E (RHE) = E (Hg/HgO) + (0.098 + 0.059 pH) V. Polarization curves were obtained using linear sweep voltammetry with a scan rate of 5 mV s^{-1}. All experiments were carried out at room temperature (~25 °C).

Determination of Faradaic efficiency (FE): Oxygen from anodic water oxidation was confirmed by gas chromatography (GC) analysis and quantified via a calibrated pressure sensor to monitor the pressure change in the anode compartment of a H-type electrolytic cell. FE was calculated by comparing the amount of experimentally measured oxygen generated by potentiostatic anodic electrolysis with theoretically calculated oxygen (assuming 100% FE). GC analysis was carried out on GC-2014C (Shimadzu Co.) with thermal conductivity detector and nitrogen carrier gas. Pressure data during electrolysis were recorded using a CEM DT-8890 Differential Air Pressure Gauge Manometer Data Logger Meter Tester with a sampling interval of 1 point per second.

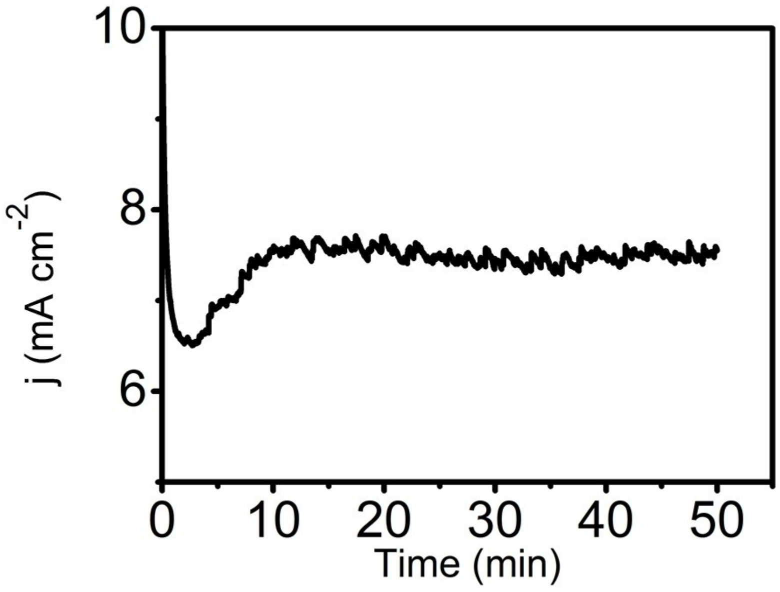

Fig. S1. Time-dependent current density curve for oxidative polarization.

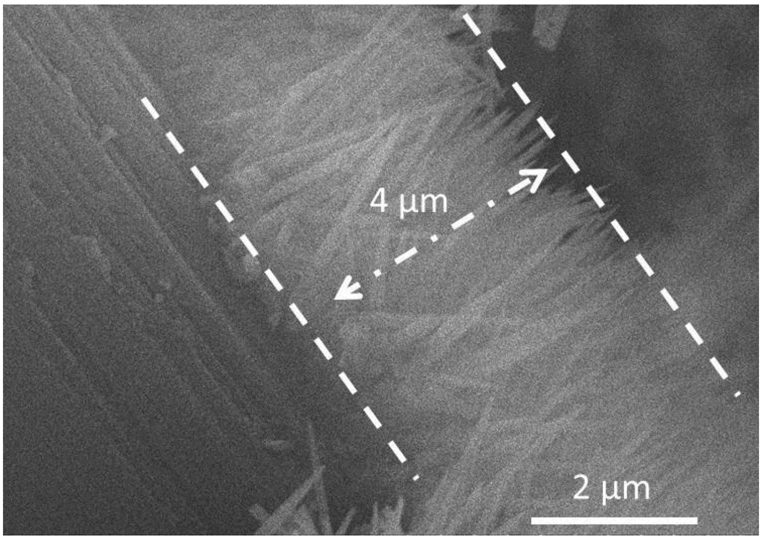

Fig. S2. The cross-sectional SEM image of $NiCo_2O_4$@Ni-Co-B/CC

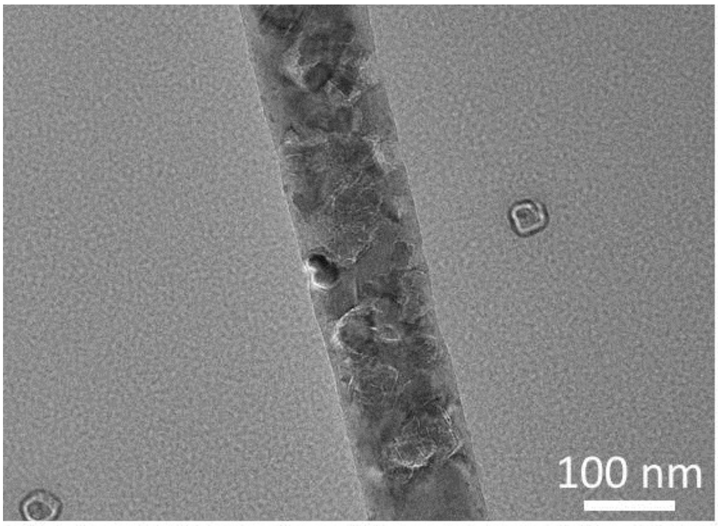

Fig. S3. TEM image of $NiCo_2O_4$@ Ni-Co-B nanowire

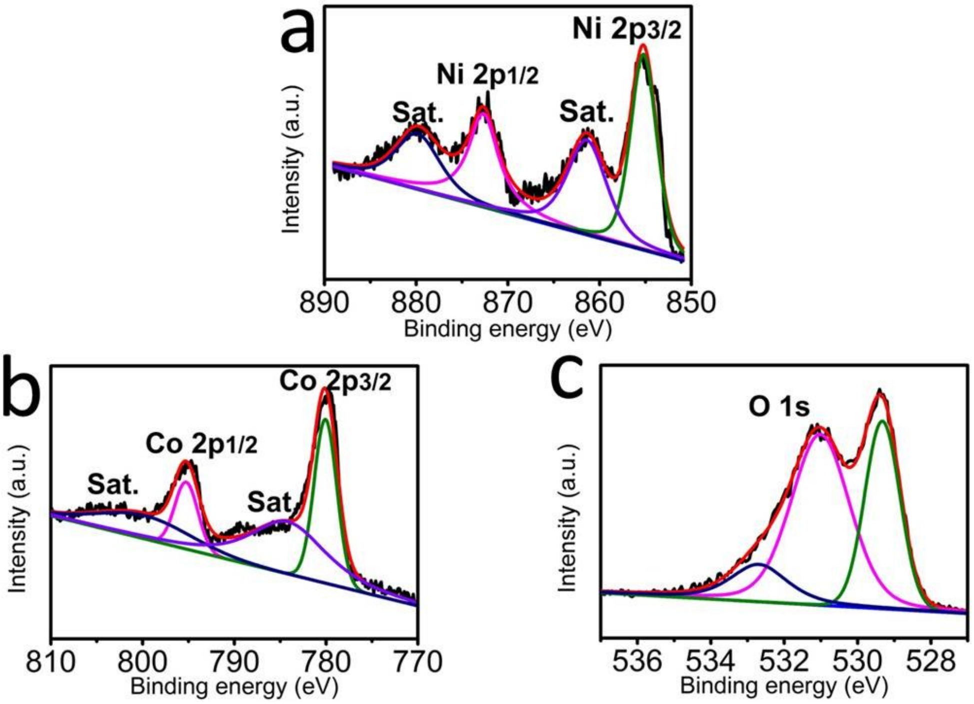

Fig. S4. XPS spectra for $NiCo_2O_4$ in the (a) Ni 2p, (b) Co 2p and (c) O 1s regions.

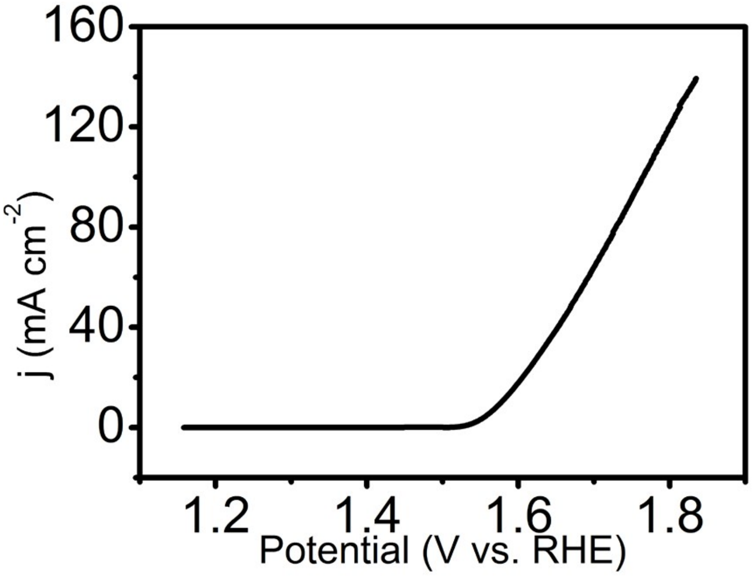

Fig. S5. LSV curve for $NiCo_2O_4$@Ni-Co-B/CC in 0.1 M KOH.

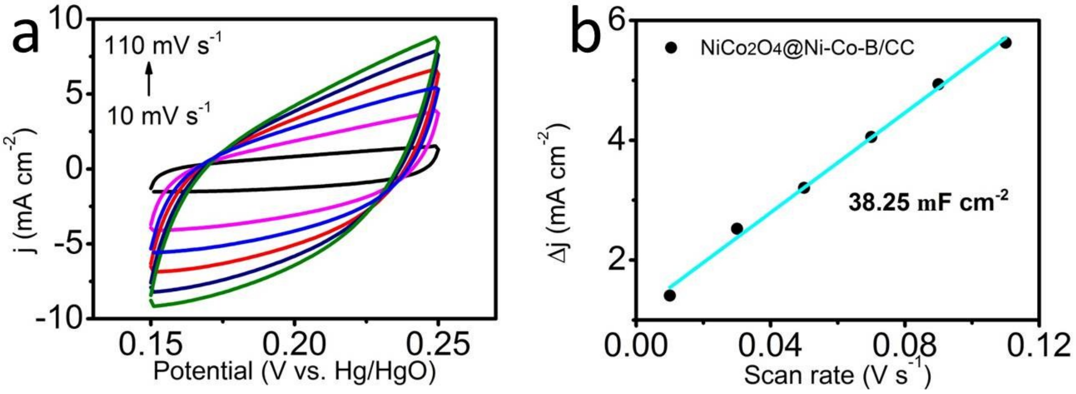

Fig. S6. (a) Cyclic voltammograms for NiCo$_2$O$_4$@Ni-Co-B/CC in the non-faradaic capacitance current range at scan rates of 10, 30, 50, 70, 90 and 110 mV s^{-1}. (b) The capacitive currents at 0.2 V vs. HgO/HgO as a function of scan rates for NiCo$_2$O$_4$@Ni-Co-B/CC.

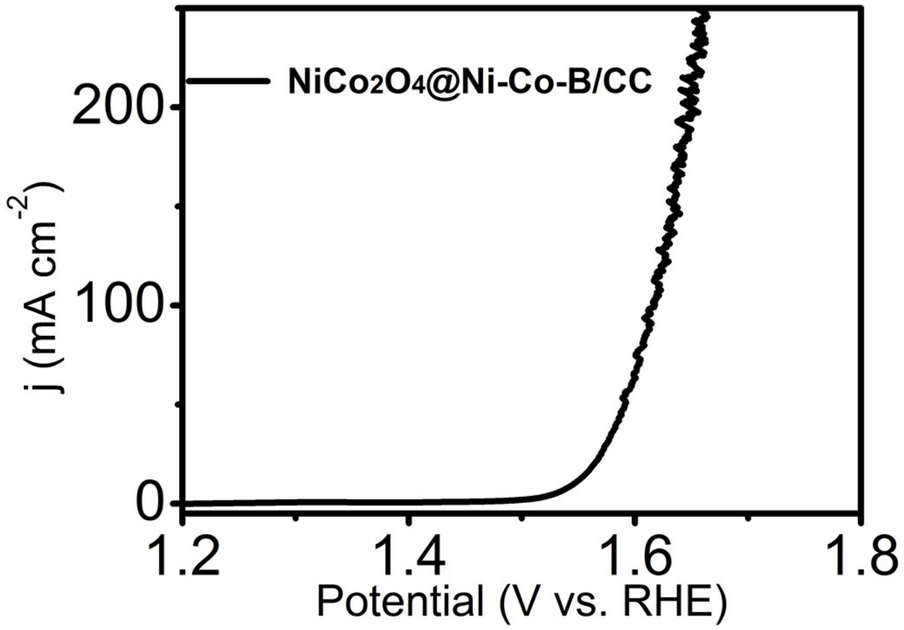

Fig. S7. LSV curve normalized by ECSA for $NiCo_2O_4$@Ni-Co-B/CC in 1.0 M KOH.

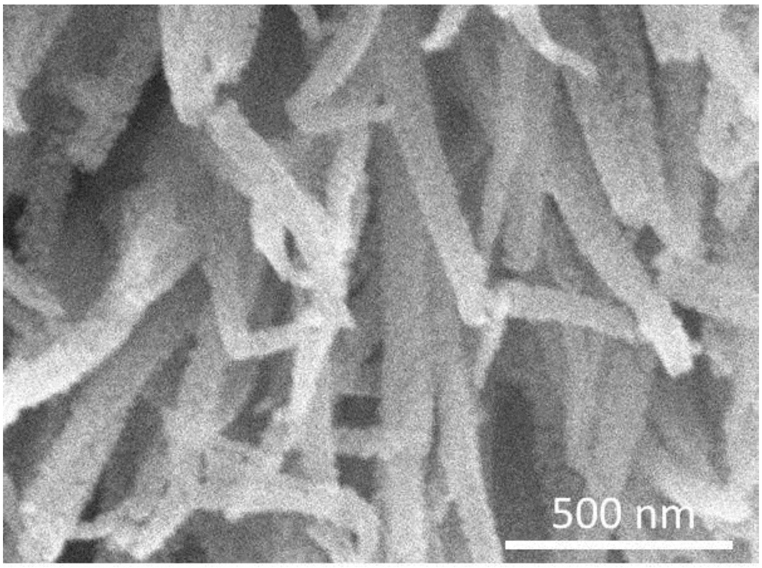

Fig. S8. SEM image of $NiCo_2O_4$@Ni-Co-B/CC after stability test in 1.0 M KOH.

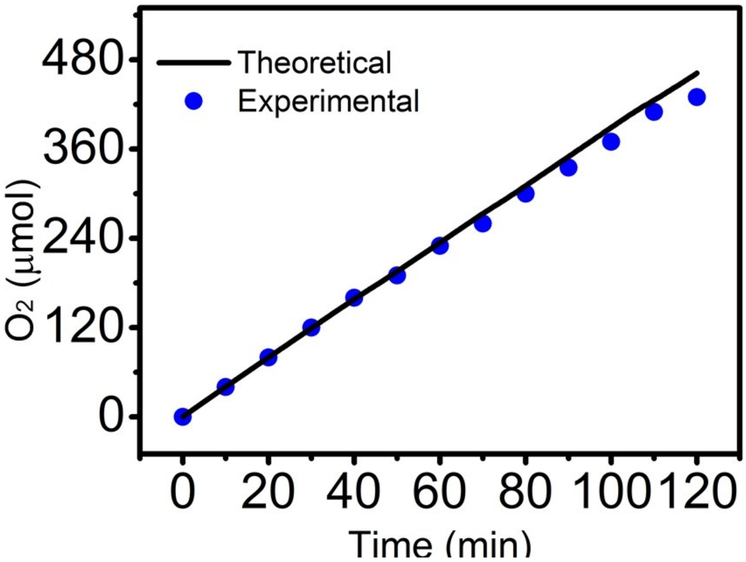

Fig. S9. The amount of oxygen theoretically calculated and experimentally measured versus time for $NiCo_2O_4$@Ni-Co-B/CC in 1.0 M KOH.

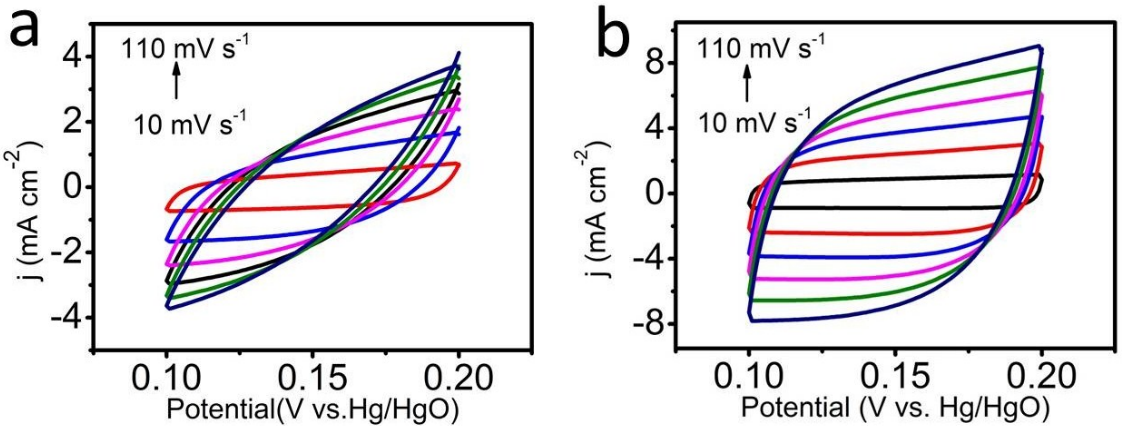

Fig. S10. Cyclic voltammograms for (a) post-OER $NiCo_2O_4$/CC and (b) post-OER $NiCo_2O_4$@Ni-Co-B/CC in the non-faradaic capacitance current range at scan rates of 10, 30, 50, 70, 90 and 110 mV s^{-1}.

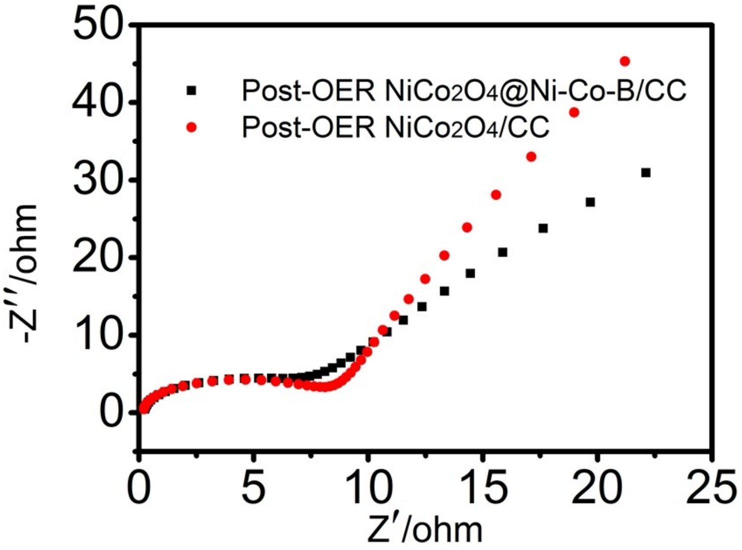

Fig. S11. Nyquist plots of post-OER $NiCo_2O_4$/CC and post-OER $NiCo_2O_4$@Ni-Co-B/CC.

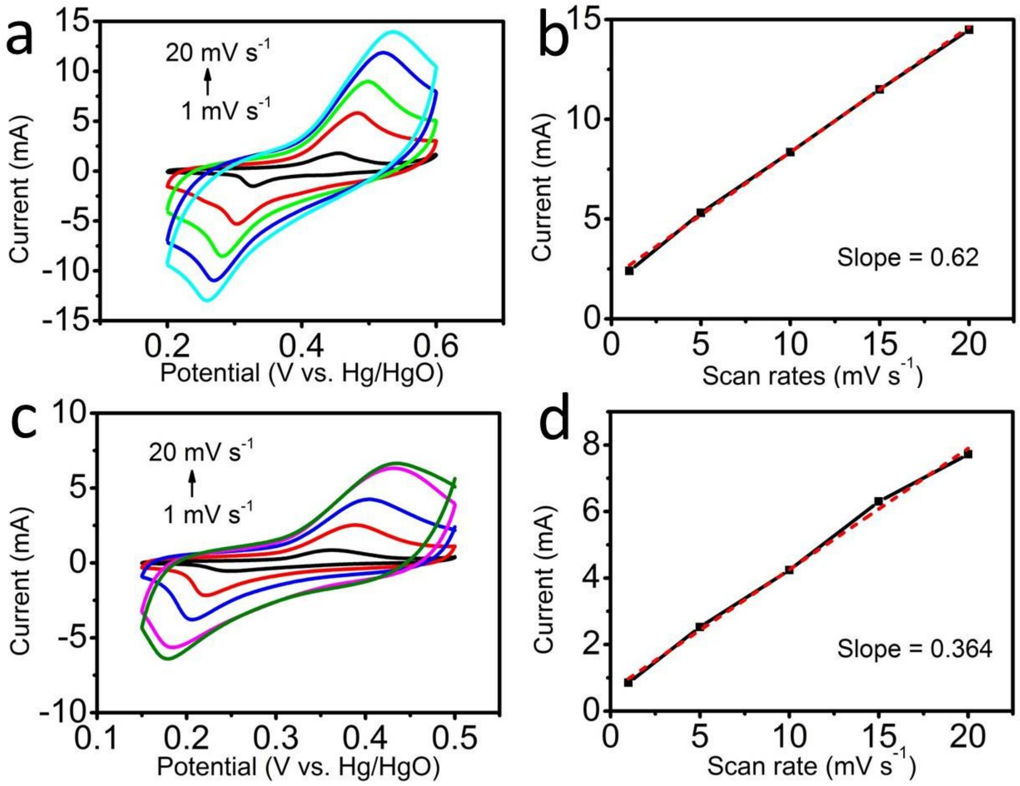

Fig. S12. (a) Cyclic voltammograms of post-OER $NiCo_2O_4$@Ni-Co-B/CC at different scan rates. (b) Linear relationship of the peak current for oxidation wave at the scan rate for post-OER $NiCo_2O_4$@Ni-Co-B/CC. (c) Cyclic voltammograms of post-OER $NiCo_2O_4$/CC at different scan rates. (d) Linear relationship of the peak current of oxidation wave at the scan rate for post-OER $NiCo_2O_4$/CC.

Table S1. Comparison of OER performance for $NiCo_2O_4$@Ni-Co-Bi/CC with other non-noble-metal electrocatalysts in alkaline media.

Catalyst	j (mA cm^{-2})	Overpotential (mV)	Electrolyte	Ref.
$NiCo_2O_4$@Ni-Co-B/CC	10	340	0.1 M KOH	This work
	20	370		
	10	270	1.0 M KOH	
	100	340		
$NiCo_2O_4$ hollow microcuboids	10	290	1.0 M KOH	2
Co_3O_4/$NiCo_2O_4$ double-shelled nanocages	10	340	1.0 M KOH	3
Au/$NiCo_2O_4$ arrays/Ti foil	10	360	1.0 M KOH	4
$NiCo_2O_4$ nanoneedles/FTO	10	323	1.0 M KOH	5
$Ni_XCo_{3-X}O_4$ nanowires	10	335	1.0 M KOH	6
Graphene- $NiCo_2O_4$ hybrid	10	390	0.1 M KOH	7
$Ni_XCo_{3-X}O_4$ nanowires	10	400	1.0 M NaOH	8
$NiCo_2O_4$ nanosheets/CNTs	10	416	1.0 M KOH	9
Au/$NiCo_2O_4$ on graphene-like material	5	377	0.1 M KOH	10
$NiCo_2O_4$ core-shell nanowires	10	320	1.0 M NaOH	11
$NiCo_2O_4$ with rich oxygen vacanies	10	320	1.0 M KOH	12

Core-ring structured $NiCo_2O_4$	100	315	1.0 M KOH	13
Porous $NiCo_2O_4$ nanosheets	20	380	0.1 M KOH	14
Co_3O_4 NW/CFP	10	330	1.0 M KOH	15
Co_3O_4/N-rmGO	10	310	1.0 M KOH	16
Fe/mCo_3O_4	10	380	1.0 M KOH	17
Co_3O_4/SWNTs	10	570	1.0 M KOH	18
Co_3O_4	10	340	1.0 M KOH	19
Mesoporous Co_3O_4	10	476	1.0 M KOH	20
N-CG–CoO	10	340	1.0 M KOH	21
NiO on Ni foam	10	440	1.0 M KOH	22
β-$Ni(OH)_2$ nanosheets	10	415	1.0 M KOH	23
Ni/NiO	10	345	1.0 M KOH	24
β-$Ni(OH)_2$	10	340	1.0 M KOH	25

References

1 J. C. Cruz, V. Baglio, S. Siracusano, V. Antonucci, A. S. Aricò, R. Ornelas, L. Ortiz-Frade, G. Osorio-Monreal, S. M. Durón-Torres and L. G. Arriaga, *Int. J. Electrochem. Sci.*, 2011, **6**, 6607-6619.

2 X. Gao, H. Zhang, Q. Li, X. Yu, Z. Hong, X. Zhang, C. Liang and Z. Lin, *Angew. Chem., Int. Ed.,* 2016, **55**, 6290-6294.

3 H. Hu, B. Guan, B. Xia and X. Lou, *J. Am. Chem. Soc.,* 2015, **137**, 5590-5595.

4 X. Liu, J. Liu, Y. Li, Y. Li and X. Sun, *ChemCatChem,* 2014, **6**, 2501-2506.

5 H. Shi and G. Zhao, *J. Phys. Chem. C,* 2014, **118**, 25939-25946.

6 X. Yan, K. Li, L. Lyu, F. Song, J. He, D. Niu, L. Liu, X. Hu and X. Chen, *ACS Appl. Mater. Interfaces,* 2016, **8**, 3208-3214.

7 S. Chen and S. Qiao, *ACS Nan,o* 2013, **7**, 10190-10196.

8 Y. Li, P. Hasin and Y. Wu, *Adv. Mater.,* 2010, **22**, 1926-1929.

9 H. Cheng, Y. Su, P. Kuang, G. Chen and Z. Liu, *J. Mater. Chem. A,* 2015, **3**, 19314-19321.

10 W. Xia, N. Li, Q. Li, K. Ye and C. Xu, *Sci. Rep.,* 2016, **6**, 23398.

11 R. Chen, H. Y. Wang, J. Miao, H. Yang and B. Liu, *Nano Energy,* 2015, **11**, 333-340.

12 J. Bao, X. Zhang, B. Fan, J. Zhang, M. Zhou, W. Yang, X. Hu, H. Wang, B. Pan and Y. Xie, *Angew. Chem., Int. Ed.,* 2015, **54**, 7399-7404.

13 B. Cui, H. Lin, J. Li, X. Li, J. Yang and J. Tao, *Adv. Funct. Mater.,* 2008, **18**, 1440-1447.

14 C. Zhu, S. Fu, D. Du and Y. Lin, *Chem. Eur. J.,* 2016, **22**, 4000-4007.

15 H. Xia, Z. Peng, L. Cuncai, Y. Zhao, J. Hao and Z. Huang, *J. Chem. Sci.,* 2016, **128**, 1879-1885.

16 Y. Liang, Y. Li, H. Wang, J. Zhou, J. Wang, T. Regier and H. Dai, *Nat. Mater.,* 2011, **10**, 780-786.

17 C. Xiao, X. Lu and C. Zhao, *Chem. Commun.*, 2014, **50**, 10122-10125.

18 J. Wu, Y. Xue, X. Yan, W. Yan, Q. Cheng and Y. Xie, *Nano Res.,* 2012, **5**, 521-530.

19 Y. Liu, G. Han, X. Li, B. Dong, X. Shang, W. Hu, Y. Chai, Y. Liu and C. Liu, *Int. J. Hydrogen Energy,* 2016, **41**, 12976-12982.

20 H. Tüysüz, Y. J. Hwang, S. B. Khan, A. M. Asiri and P. Yang, *Nano Res.,* 2013, **6**, 47-54.

21 S. Mao, Z. Wen, T. Huang, Y. Hou and J. Chen, *Energy Environ. Sci.,* 2014, **7**, 609-616.

22 G. Han, Y. Liu, W. Hu, B. Dong, X. Li, X. Shang, Y. Chai, Y. Liu and C. Liu, *Appl. Surf. Sci.,* 2015, **359**, 172-176.

23 H. Liang, L. Li, F. Meng, L. Dang, J. Zhuo, A. Forticaux, Z. Wang and S. Jin, *Chem. Mater.,* 2015, **27**, 5702-5711.

24 J. Liang, Y. Wang, C. Wang and S. Lu, *J. Mater. Chem. A,* 2016, **4**, 9797-9806.

25 S. C. Jung, S. L. Sim, Y. W. Soon, C. M. Lim, P. Hing and J. R. Jennings, *Nanotechnol.,* 2016, **27**, 275401.